Journal of Photochemistry and Photobiology A: Chemistry 211 (2010) 115–122

Contents lists available at ScienceDirect

Journal of Photochemistry and Photobiology A: Chemistry

journal homepage: www.elsevier.com/locate/jphotochem

Rod-like pyrene–perylene bisimide molecular triads: Synthesis and photophysical properties

Jun-Hua Wan[a], Zhun Ma[b], Feng Liu[b], Zheng Xu[a], Hong-Yu Wang[b], Hong-Ji Jiang[c], Wei Huang[c,*]

[a] Key Laboratory of Organosilicon Chemistry and Material Technology of Ministry of Education, Hangzhou Normal University, Hangzhou 310012, China
[b] Institute of Advanced Materials, Fudan University, Shanghai 200433, China
[c] Institute of Advanced Materials (IAM), Nanjing University of Posts and Telecommunications (NUPT), 66 XinMoFan Road, Nanjing 210003, China

ARTICLE INFO

Article history:
Received 1 November 2009
Received in revised form 21 January 2010
Accepted 12 February 2010
Available online 21 February 2010

Keywords:
Pyrene
Perylene bisimide
Energy transfer
Molecular triad
Linker

ABSTRACT

Two rod-like pyrene–perylene bisimide triads with different linkers were synthesized and characterized. Their photophysical properties were investigated by UV–vis absorption, both steady-state and time-resolved emission. According to fluorescence excitation and time-resolved emission spectroscopic studies, efficient intramolecular resonance energy transfer was observed in both triads. Furthermore, the influence of the molecular structure on the energy transfer rates was also studied and discussed. To gain insights into the intramolecular interactions and the electronic structures, the electronic structures of both triads were investigated through theoretical calculation.

1. Introduction

Design and synthesis of multicomponent molecules have attracted much attention in the last two decades because of their applications in artificial photosynthesis systems [1–2], molecular machines [3–4], and optoelectronic devices [5–6]. One of the interesting photophysical properties of the multicomponent molecules is the highly efficient electron/energy transfer processes produced by hybridization of different photoactive or redox-active chromophores [7–10]. The induced intramolecular energy transfer process can be adopted to extend the "virtual" Stokes' shift for fluorescent sensing and biochemical applications [11–13], whilst the electron transfer process is crucial to create long-lived charge-separated states for photovoltaic application [14–16].

During the past few years, perylene bisimide (**Per**) dyes have been investigated widely as building blocks for photoactive systems, owing to their good thermal and photochemical stability, high electron affinity, and fluorescence quantum yield of almost unity [17–20]. Pyrene (**Py**) is another widely studied fluorophore as a building block due to its durable electronic properties and long excited singlet lifetimes [21–25]. Recently, several flexibly linked pyrene–perylene bisimide-based bichromophoric systems were synthesized [26–27]. Furthermore, effective energy and electron transfer processes were observed in these systems. These observations open the door to investigations on pyrene–perylene bisimide systems for the realization of corresponding optoelectronic devices (such as photovoltaic cells). The rod-like pyrene–perylene bisimide systems, however, have not received much attention [28–30]. The fixed donor–acceptor distance and orientation in rod-like systems would be expected to produce an obvious influence on photo-induced processes [31–32]. Additionally, a highly rigid molecule with a donor–acceptor structure would be useful in studying intermolecular interactions by self-assembly [33].

In this paper we describe the synthesis and photophysical properties of a bichromophoric system containing the bay-functionalized perylene bisimide moiety as the acceptor and two pyrene moieties as donors. Two pyrene moieties are linked to the perylene bisimide core via phenylene linkers to form a triad structure (**Py-Per-Py**) (see Scheme 1). This rigid structure compared to the flexibly linked pyrene–perylene bisimide system could produce a distinct effect on photophysical behavior and photo-induced reactions. In another pyrene–perylene bisimide system (**Py-e-Per-e-Py**), pyrene moieties are connected with the perylene bisimide core by way of phenylethyne linkers. For this triad, the pyrene moieties are expected to rotate freely around the ethylene bond. Introduction of the ethylene bond produced interesting differences in the photophysical and photo-induced processes between the two different triads. The monolayer assembly and electronic states

* Corresponding author. Tel.: +86 025 85866396/85866360; fax: +86 025 85866396.
E-mail addresses: wei-huang@njupt.edu.cn, iamdirector@fudan.edu.cn (W. Huang).

1010-6030/$ – see front matter © 2010 Elsevier B.V. All rights reserved.
doi:10.1016/j.jphotochem.2010.02.006

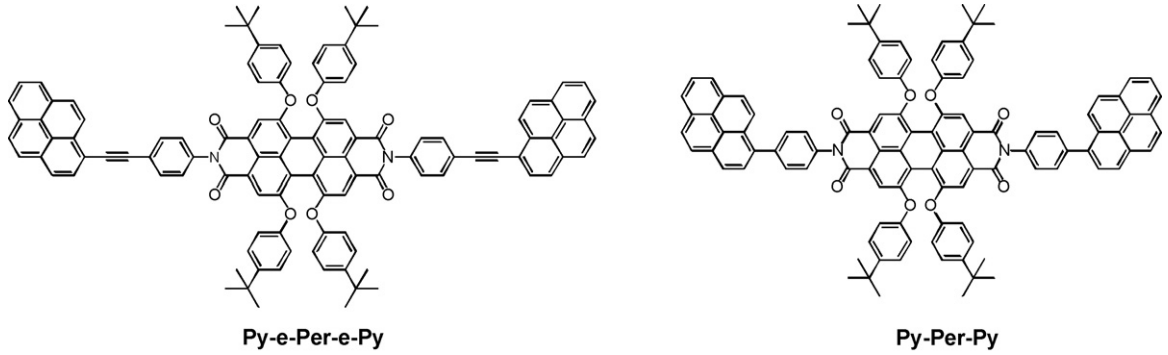

Scheme 1. Structures of triads.

for the two triads have also been investigated by scanning tunneling microscopy and spectroscopy (STM/STS) at the liquid/solid interface [34].

2. Experimental

2.1. Materials and equipment

All of the chemicals and reagents were purchased from a commercial supplier and used without further purification. The solvents (THF and CH_2Cl_2) were dried according to standard methods. Compound **1** [35] and **2** [36–37] were synthesized according to the literature.

^1H and ^{13}C NMR spectra were collected on 400 MHz and 100 MHz spectrometers, respectively, with tetramethylsilane as the internal standard. Matrix-assisted laser desorption ionization-time-of-flight (MALDI-TOF) mass spectrometry experiments were carried out using a Shimadzu AXIMA–CFRTM Plus time-of-flight mass spectrometer (Kratos Analytical, Manchester, UK). UV–vis spectra were recorded on a Shimadzu 3150 PC spectrophotometer. Steady-state emission experiments were carried out on a Shimadzu RF-5301 PC spectrophotometer with a xenon lamp as a light source.

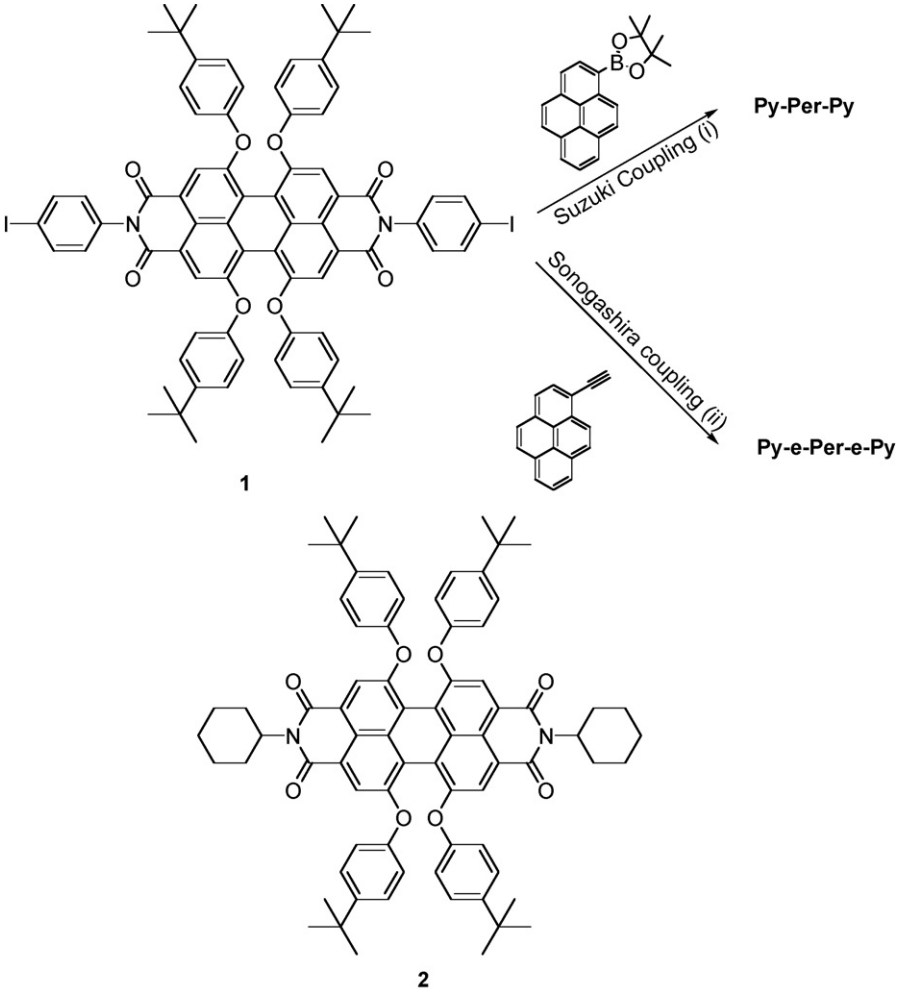

Scheme 2. Reaction conditions: (i) $Pd(PPh_3)_4$, 1 M Na_2CO_3/THF, 50 °C; (ii) $Pd(PPh_3)_4$/CuI, Et_3N/THF, 80 °C.

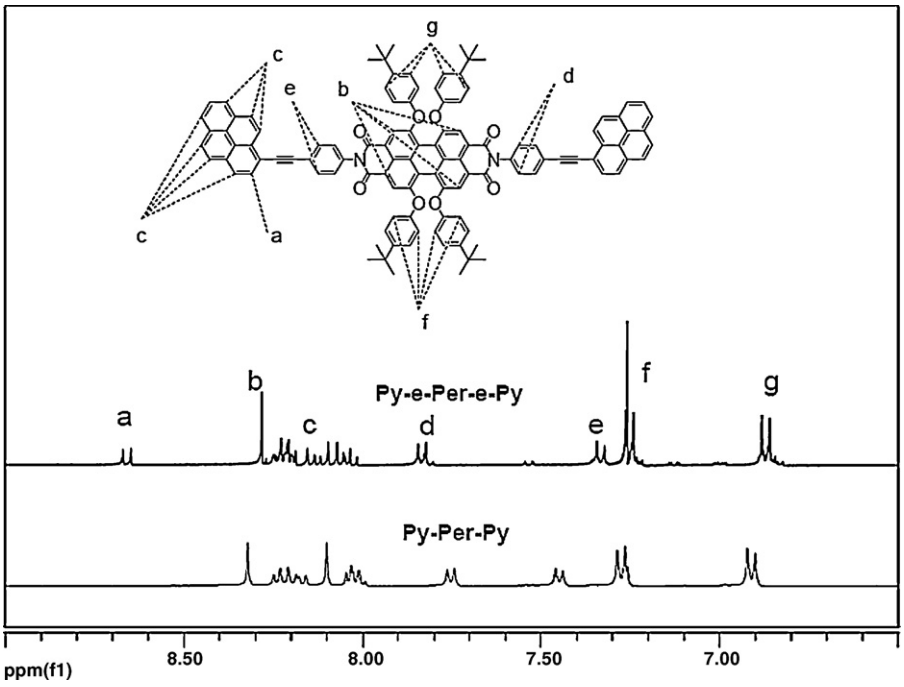

Fig. 1. ^{1}HNMR spectra in the aromatic range for the two triads.

Time-resolved emission studies were performed with an Edinburgh FL 920 photon counting system with a hydrogen-filled lamp as the excitation source. The data were analyzed by iterative convolution of the luminescence decay profile with the instrument response function, using a software package provided by Edinburgh Instruments.

2.2. Molecular orbital calculations

All geometries were initially optimized with MM2 method combined in ChemBioOffice 2008 with default set, and then by the semi-empirical AM1 method. The obtained optimized geometries were finally re-optimized with ab initio HF method at 3–21 g level. The frontier orbitals were depicted with 0.01 isocontour based on HF/3–21 g level. All the calculation is done using Gaussian 03 software package.[38]

2.3. Synthesis

2.3.1. ***Py-Per-Py***

A mixture of 1-pyrene boronic ester (97 mg, 0.3 mmol), compound **1** (138 mg, 0.1 mmol), and $Pd(PPh_3)_4$ (15 mg, 0.013 mmol) catalyst in 5 mL of 1 M aqueous K_2CO_3 solution and THF (v/v, 1:1) was placed in a two-necked, round-bottom flask fitted with a condenser. The entire setup was degassed and back-filled with a gaseous mixture of argon. Then the reaction mixture was heated to reflux for 24 h. After being cooled to room temperature, the mixture was extracted with 10 mL of $CHCl_3$ three times. The combined organic phase was washed with brine, dried over $MgSO_4$, and concentrated. The residue was purified by column chromatography using a mixture of dichloromethane/petroleum ether (1:1) as eluent to give the product as a deep red solid (87 mg). Isolated yield: 57%. ^{1}H NMR (400 MHz, $CDCl_3$) δ 8.32 (s, 4H), 8.24–8.15 (m, 8H), 8.10 (s, 4H), 8.04–8.01 (m, 6H), 7.76–7.74 (d, 4H), 7.45–7.43 (d, 4H), 7.28–7.25 (d, 8H), 6.92–6.90 (d, 8H), 1.25 (s, 36H). ^{13}C NMR (100 MHz, $CDCl_3$) δ 164.0, 156.4, 153.0, 147.7, 141.8, 136.9, 134.5, 133.2, 131.6, 131.2, 131.0, 128.7, 127.8, 126.9, 126.2, 125.4, 125.1, 125.0, 124.8, 122.7, 121.0, 120.4, 119.6, 53.6, 34.6, 31.0. MASS (MALDI-TOF, dithranol): 1535.1 (calcd. for $C_{102}H_{82}N_2O_8$: 1535.8).

2.3.2. ***Py-e-Per-e-Py***

A mixture of compound **1** (138 mg, 0.1 mmol), $Pd(PPh_3)_4$ (15 mg, 0.013 mmol) and CuI (3 mg, 0.016 mmol) was placed in a two-necked, round-bottom flask fitted with a condenser. The entire setup was degassed and back-filled with a gaseous mixture of argon. To the reaction flask was added previously degassed 5 mL of THF and TEA (10 ml) using syringes. The 1-ethylenepyrene (68 mg, 0.3 mmol) was dissolved in 5 mL of THF and added to the reaction mixture at about 60 °C (bath temperature). The reaction mixture was then stirred at reflux overnight under the atmosphere of the gas mixture. The solvents were evaporated and the residue was purified by column chromatography using dichloromethane/petroleum ether (1:1) as eluent to give the product as a purple solid (73 mg). Isolated yield: 46%. ^{1}H NMR (400 MHz, $CDCl_3$) δ 8.67–8.64 (d, 2H), 8.28 (s, 4H), 8.40–8.03 (m, 16H), 7.84–7.82 (d, 4H), 7.34–7.32 (d, 4H), 7.25–7.24 (d, 8H), 6.88–6.85 (m, 8H), 1.25 (s, 36H). ^{13}C NMR (100 MHz, $CDCl_3$) δ 163.7, 156.3, 153.0, 147.7, 139.5, 137.2, 133.4, 132.7, 132.2, 131.6, 129.9, 129.0, 128.6, 127.5, 126.9, 126.5, 125.9, 124.7, 122.6, 121.0, 120.4, 119.5, 117.9, 94.5, 89.8, 34.6, 31.2, 29.9. MASS (MALDI-TOF, dithranol): 1583.1 (calcd. for $C_{112}H_{82}N_2O_8$: 1583.8).

3. Result and discussion

3.1. Synthesis

Scheme 2 shows the synthetic routes of both triads. The approach to the synthesis of the target molecules **Py-Per-Py** and **Py-e-Per-e-Py** involves palladium-catalyzed coupling reactions. *N*,*N*′-i-4-iodiobenzene-1,6,7,12-tetrakis(4-t-butyl-pheoxy)-3,4:9,10-tetracarboxdiimide (**1**) was selected as the perylene building block due to its good solubility and ease of synthesis. After precipitating from methanol, **Py-Per-Py** was obtained with 57% yield by coupling compound **1** with 1-pyreneboronic acid ester by the Suzuki coupling reaction. **Py-e-Per-e-Py** was

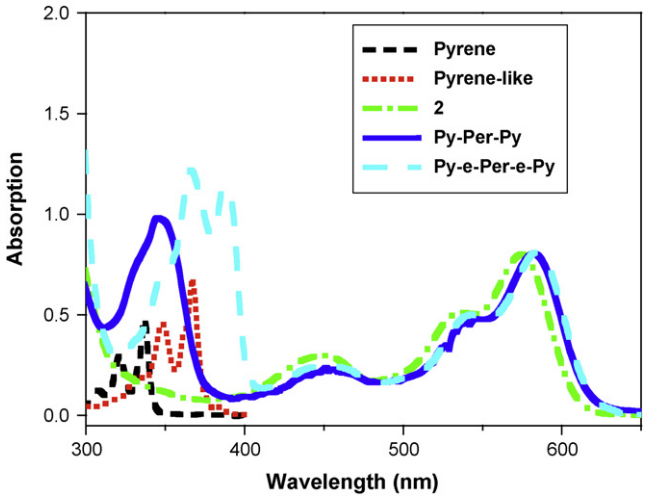

Fig. 2. The absorption spectra for the two triads, compound **2**, pyrene and pyrene-like monomer (1-trimethylsilylacetylenepyrene) in CH_2Cl_2 (1×10^{-5} M).

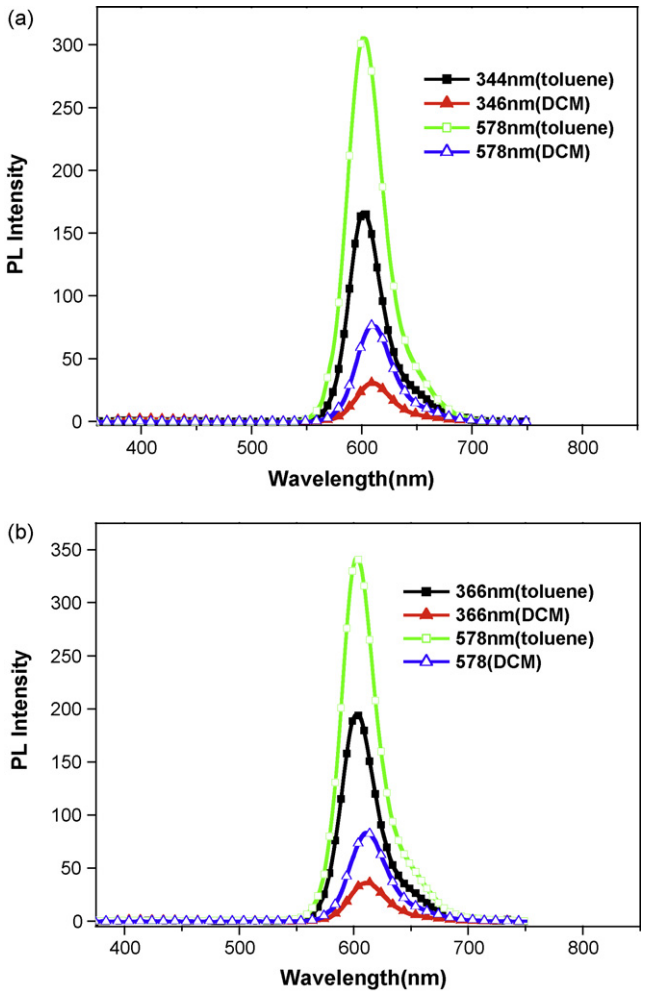

Fig. 3. The emission spectra for the two triads in toluene and CH_2Cl_2. (1×10^{-5} M) (a) for **Py-Per-Py** and (b) for **Py-e-Per-e-Py**.

prepared through the Sonogashira coupling reaction. In the first step, the 1-ethynylpyrene building block was synthesized from 1-bromopyrene by a Sonogashira coupling with trimethylsilylacetylene [39]. Our initial attempt to synthesize **Py-e-Per-e-Py** through cross-coupling of 1-ethynylpyrene with compound **1** under the Sonogashira reaction conditions led to self-coupling of 1-ethynylpyrene to give the corresponding dimer in unacceptable yield [40]. It is well-known that self-coupling of terminal alkynes usually occurs as a side-reaction alongside cross-coupling [41–42]. The ethyne-linked pyrene dimer was not easy to remove by column chromatography due to its low solubility in common solvents. To reduce the self-coupling reaction, the procedure of reagent addition was also changed. The solution of 1-ethylenepyrene in anhydrous THF was added slowly to the reaction mixture at refluxing temperature by a syringe. Following this improved method, **Py-e-Per-e-Py** was obtained by coupling 1-ethynylpyrene with **I-Per-I**, in the presence of $Pd(PPh_3)_4$/CuI in THF/Et_3N (v/v = 1:1), with isolated yields of 46%.

The structure and purity of the two triads were verified by ^1H and ^{13}C NMR, MALDI-TOF MS. The fingerprint of these molecules was given by the ^1HNMR spectra. In particular, for **Py-e-Per-e-Py** a doublet was found at 8.67 ppm, corresponding to the proton located at the 2-position of the two pyrene moieties. Both triads exhibited a characteristic single signal at around 8.30 ppm (8.32 ppm for **Py-Per-Py** and 8.28 ppm for **Py-e-Per-e-Py)**. In both cases, the singlet can be attributed to the perylene moiety. The multiple signals between 8.4 to 8.0 ppm were assigned to the other protons of pyrene moieties for both triads (see Fig. 1). It is noteworthy that the quaternary ethynyl carbon that resonates at 94.5 and 89.8 ppm for **Py-e-Per-e-Py** in ^{13}C NMR spectra was identified.

3.2. Optical properties

3.2.1. Steady-state spectroscopy

Spectroscopic properties of the two triads were investigated with UV–vis absorption, excitation and fluorescence emission. The absorption spectra of two triads and corresponding monomers in CH_2Cl_2 solutions are depicted in Fig. 2, and the absorption data are summarized in Table 1. Both triads exhited several absorption bands. For **Py-Per-Py**, the absorption bands in the longer wavelength range (above 400 nm) came from the perylene bisimide moiety [43–44]: 447 nm (belonging to the S_0–S_2 electronic tran-

Table 1
The photophysical properties for two triads.

Compound	Solvents	Absorption (nm)[a]	Emission[b]			
			λ (nm)	λ (nm)	τ_{Py}[c] (ns)	τ_{Per}[c] (ns)
Py-Per-Py	Toluene	344, 445, 534, 578	400	602	3.25	4.07
	DCM	346, 447, 540, 582	400	610	1.13	1.19
Py-e-Per-e-Py	Toluene	366, 390, 447, 537, 578		602	3.50	7.58
	DCM	366, 386, 452, 541, 582	400	610	1.13	1.06
2	DCM	448, 537, 573		610		6.53[d]

[a] Measured in solution (1×10^{-5} M).
[b] The excitation wavelengths are 344 (toluene) and 346 (DCM) nm for **Py-Per-Py**, 366 nm for **Py-e-Per-e-Py**.
[c] The excitation wavelength is 370 nm.
[d] Cited from Ref. [35].

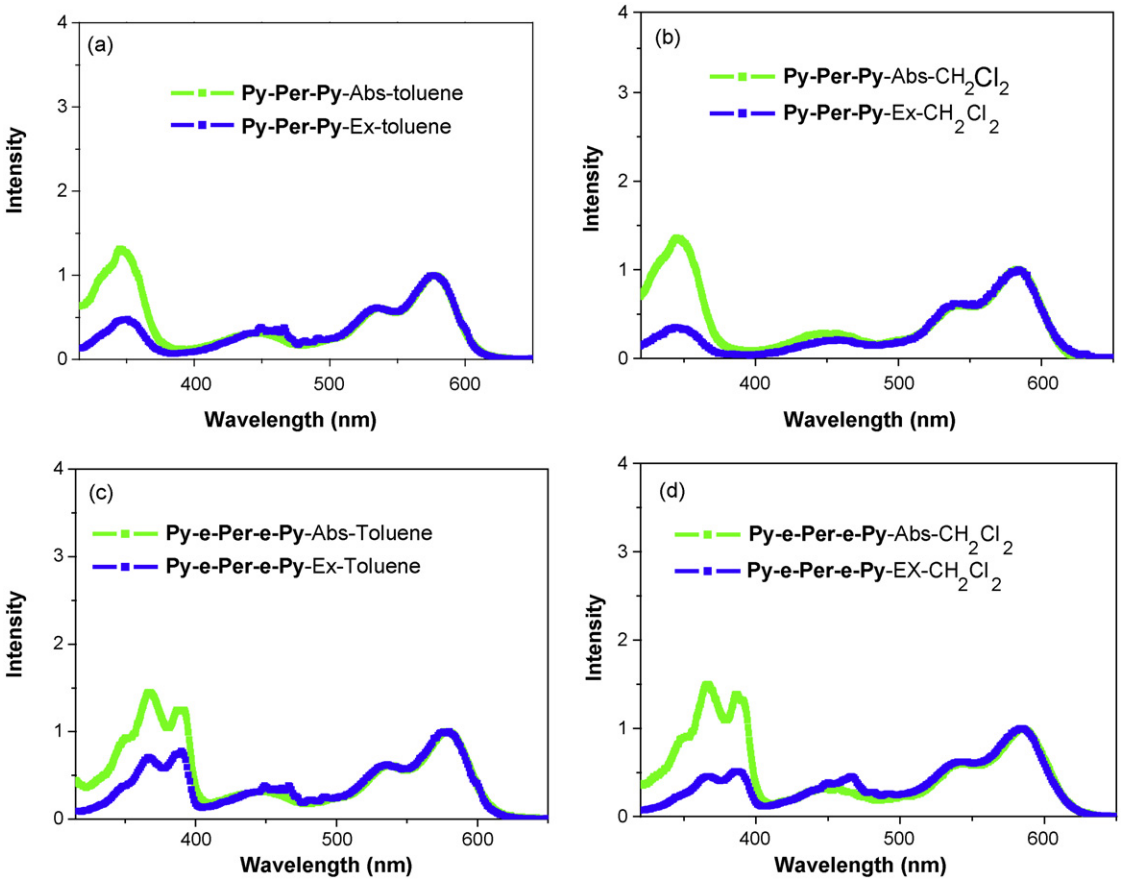

Fig. 4. UV/Vis absorption (green line) and fluorescence excitation spectra (blue line, λ_{ex} = 602 nm in toluene and 610 nm in CH_2Cl_2, respectively), (a) and (b) for **Py-Per-Py** in toluene and CH_2Cl_2 solution, respectively; (c) and (d) for **Py-e-Per-e-Py** in toluene and CH_2Cl_2 solution, respectively.

sition), 540 and 582 nm (belonging to S_0–S_1 electronic transition). The other absorption band (346 nm) came from the π–π transition of the pyrene moieties. Surprisingly, the absorption of the pyrene moiety in this triad was obviously different from that of the pyrene monomer, and exhibited no fine structure besides the minor bathochromic shift of 9 nm for the absorption of the perylene moiety. The vibration fine structure in **Py-Per-Py** system is destroyed by swinging for aromatic ring around the C(Py)-C(pheny) bond. **Py-e-Per-e-Py** had almost the same absorption spectrum for the perylene moiety as **Py-Per-Py**; but the absorption spectrum for the pyrene moiety in **Py-e-Per-e-Py** exhibited distinct fine structures. The fine structures come from different conformers populating in solution. The conformation with pyrene and benzene rings in phenylethynylpyrene are perpendicular to each other is most stable (see Section 3.4). The other is a transition state for the rotation of an aromatic ring around C–C triple bond due to very low barrier. The absorption bands for both triads in toluene showed no remarkable differences compared with those in CH_2Cl_2.

The emission spectra of the two triads in toluene solutions at room temperature were recorded upon excitation at 344 nm for **Py-Per-Py,** and 366 nm for **Py-e-Per-e-Py**, where the corresponding pyrene-like units had a strong absorption (see Fig. 3). Both triads had an emission maximum around 602 nm, typical of the perylene moiety. However, no emissions from pyrene moieties between 360 to 500 nm were detected for both triads. This result indicates that effective energy transfer from **Py*** to **Per*** occurred. At the same time, the emission spectra of the two triads were also investigated in weakly polar solvent CH_2Cl_2. The emission maximum was slightly red-shifted (10 nm) in comparison with that in the nonpolar solvent toluene. The local excited state of Per would be relatively polar than the ground state. Hence, the small red shift of the emission may be ascribed to the stabilization of Per* by the polar solvent.

The energy transfer process could also be confirmed by the fluorescence excitation spectrum (Fig. 4). Although energy transfer was not quite complete in this system, the spectral profiles were closely comparable for them in both polar and nonpolar solvents. In the region of perylene bisimide absorption bands between 400 and 600 nm, the fluorescence excitation spectra exhibited a good match with the corresponding UV/Vis absorption spectrum, whereas a significantly reduced intensity was observed for the pyrene bands. These results indicate that another photo-induced reaction may be occur besides the energy transfer process. It is worth noting that, based on the integrated intensities from 320 to 380 nm for **Py-Per-Py** and 320 to 410 nm for **Py-e-Per-e-Py**, the energy transfer from **Py*** to **Per*** was more efficient in toluene than that in CH_2Cl_2, especially for **Py-e-Per-e-Py**. Generally, the energy transfer process is independent of the polarity of the solvent. The difference might arise from the existence of electron transfer (from **Py*** to CS–charge separation states, which is more stabilized by the polar solvent). It is expected that efficient electron transfer reactions can occur in a covalently linked donor-acceptor system, especially for the rod-like donor-acceptor-donor triads [45–47]. The emissions in different polar solvents can indirectly show the existence of this process. The emission spectra of the perylene bisimide moieties are more strongly quenched in CH_2Cl_2 compared to those in toluene for both triads upon excitation at the same wavelength (344 and 578 nm for **Py-Per-Py**, 366 and 578 nm for **Py-e-Per-e-Py**).

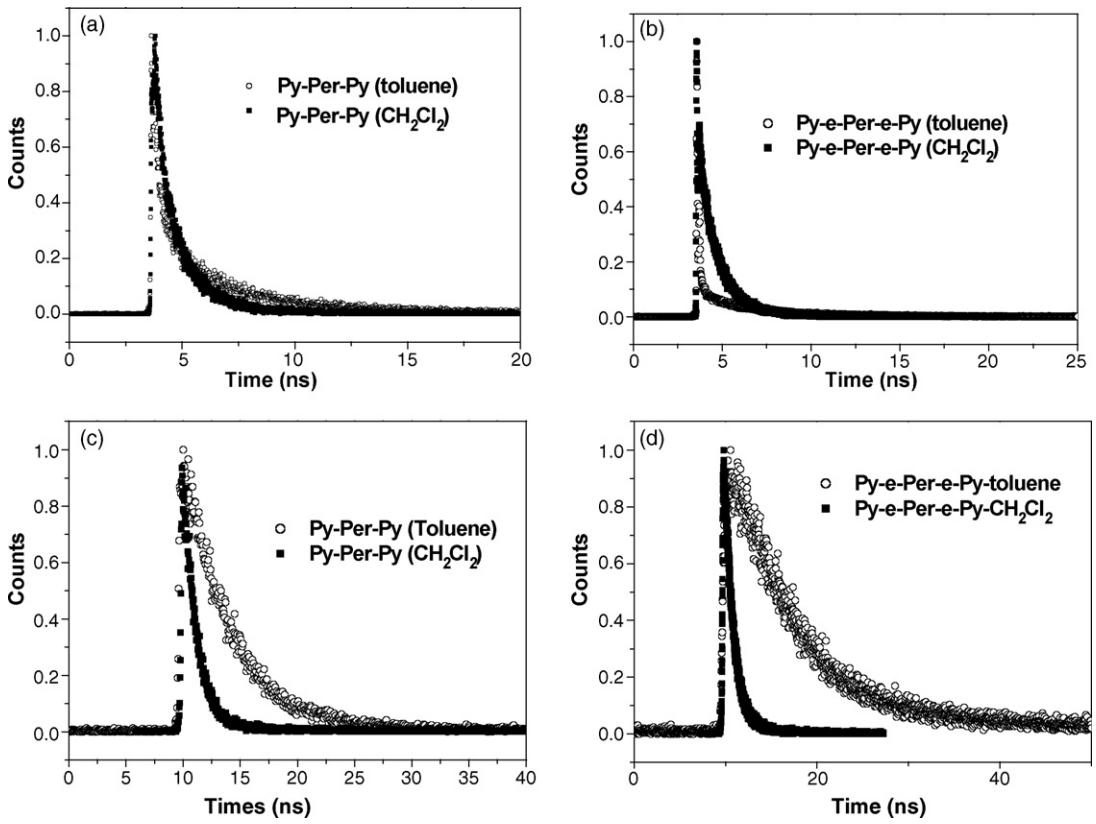

Fig. 5. Time-resolved emission of the triads in toluene and dichloromethane (λ_{ex} = 370 nm). (a) decaying lifetime of the pyrene moiety of **Py-Per-Py** measured at 400 nm; (b) decaying lifetime of the pyrene-like moiety of **Py-e-Per-e-Py** measured at 408 nm; (c) and (d) decaying lifetime of the perylene bisimide moiety of two triads measured at 602 nm in toluene and 610 nm in CH_2Cl_2, respectively.

3.2.2. Time-resolved emission

The fluorescence lifetimes for **Py-Per-Py** and **Py-e-Per-e-Py** at room temperature were recorded upon excitation at 370 nm. Fig. 5 shows the fluorescence kinetic curves of the two triads in both toluene and dichloromethane solutions (Table 1). All fluorescence lifetimes measured followed monoexponential decay. The fluorescent states associated with the pyrene moiety have remarkably shorter lifetimes than that of the pyrene monomer. On this basis, it appears that photons collected by the appended pyrene polycycles are transferred mostly to the perylene bisimide moiety. The lifetimes for the pyrene moieties, recorded at 400 nm, change in solvents of different polarity and are remarkably shorter (about 3-fold) in CH_2Cl_2 than in toluene. In the same way, the lifetimes for **Per*** of the two triads, recorded at 610 nm in CH_2Cl_2, are also much shorter in comparison with that of perylene bisimide monomer (compound **2,** 6.53 ns)[35]. This observation further suggests that the electron transfer processes may be in existence for the two triads besides energy transfer.

Table 2
Parameters used to calculate the rate constants for Förster-type energy transfer in the two triads.

Parameter	Py-Per-Py[a]	Py-e-Per-e-Py[a]
Φ_F[b]	0.65	0.86
τ_F (ns)[b]	650	55
R_{CC} (Å)[c]	13.0	14.5
J_F (10^{14} M^{-1} cm^{-1} nm^4)	1.53	1.95
R_0 (Å)	33.5	44.6
K_F (s^{-1})	4.5×10^9	4.5×10^{10}

[a] Refers to singlet energy transfer from the pyrene monomer to the S2 state localized on the perylene bisimide.
[b] Fluorescence quantum yield and lifetime for pyrene and 1-trimethylsilylacetylenepyrene.
[c] Average center-to-center separation distance derived from the optimized structures at AM1 level.

3.3. Förster energy transfer

According to the steady-state and time-resolved spectroscopic studies, there is energy transfer from **Py*** to the **Per*** in **Py-Per-Py** and **Py-e-Per-e-Py** triads. The following observations support this conclusion. (1) Both triads exhibit only one maximum emission, and this emission maximum is clearly independent of the excitation wavelength. (2) The fluorescence excitation spectra match the corresponding UV/Vis absorption spectrum in the area of the perylene bisimide absorption bands between 400 and 600 nm, in spite of a significantly reduced intensity for the pyrene bands. (3) The **Py*** lifetimes for both triads (1.13 ns in CH_2Cl_2) are much shorter than the lifetimes for the corresponding reference monomers (pyrene and 1-trimethylsilylacetylenepyrene, τ_F = 650 and 55 ns, respectively) [22,26].

For the two triads, the pyrene polycyclics are attached at two end positions of the perylene core, which are the nodes of the electronic energy level (HOMO/LUMO). The ethynylene connector in **Py-e-Per-e-Py** could not act as an effective conduit for through-bond interactions due to the node [48–49]. The dominating mechanism is intramolecular energy transfer via the through-space exchange mechanism (Förster-type energy transfer, TS). In general, the rate of energy transfer depends on the extent of spectral overlap of the emission spectrum of the donor with the absorption spectrum of the acceptor, the quantum yield of the donor, the relative orientation of the donor and acceptor transition dipoles, and the distance between the donor and acceptor molecules [50]. The rate constant (k_F) for Förster-type energy transfer can be expressed in terms of

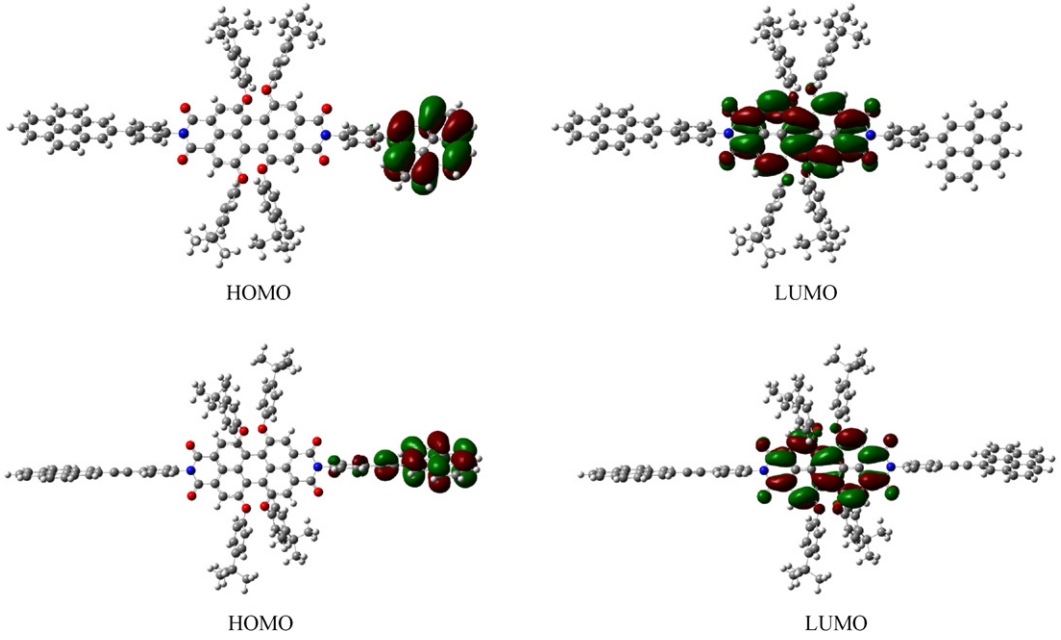

Fig. 6. Energy minimized structure calculated showing the distribution, for **Py-Per-Py**: HOMO (top left), LUMO (top right); for **Py-e-Per-e-Py**: HOMO (bottom left) and LUMO (bottom right).

Eq. (1):

$$k_F = \frac{(8.8 \times 10^{-25})\phi_F K^2}{n^4 \tau_F R_{CC}^6} J_F \quad (1)$$

where

$$J_F = \frac{\int_0^\infty F_D(\nu) \in_A(\nu) \nu^{-4} \, d\nu}{\int_0^\infty F_D(\nu) \, d\nu}$$

and n is the refractive index of the surrounding solvent (n_{DCM} = 1.4240), Φ_F refers to the quantum yield of the donor in the absence of acceptor (pyrene and 1-trimethylsilylacetylenepyrene, Φ_F = 0.65 and 0.86, respectively), τ_F is the lifetime of the donor in the absence of acceptor, R_{CC} is the center-to-center separation distance between the donor and acceptor (13 Å for **Py-Per-Py** and 14.5 Å for **Py-e-Per-e-Py,** obtained from calculations), K^2 is their mutual orientation factor, and generally assumed as 2/3 in calculations, and J_F is the spectral overlap integral of the donor emission and the acceptor absorption ($1.53 \times 10^{14}\,M^{-1}\,cm^{-1}\,nm^4$ for **Py-Per-Py** and $1.95 \times 10^{14}\,M^{-1}\,cm^{-1}\,nm^4$ for **Py-e-Per-e-Py**). The parameters used to calculate the Förster-type energy transfer rates are collected in Table 2. According to Eq. (1), the energy transfer rates for both triads can be obtained, $4.5 \times 10^9\,s^{-1}$ for **Py-Per-Py** and $4.5 \times 10^{10}\,s^{-1}$ for **Py-e-Per-e-Py** in CH_2Cl_2. The former is 10-fold smaller than the latter. Therefore, the energy transfer in **Py-e-Per-e-Py** is much quicker than that in **Py-Per-Py**.

Generally, for Förster-type energy transfer, the distance between the donor (D) and acceptor (A) plays an important role. The distance at which energy transfer is 50% efficient, called the Förster distance, is typically in the range of 20–60 Å. The Förster distance can be obtained from Eq. (2):

$$R_0 = 0.211[K^2 n^{-4} \Phi_F J_F]^{1/6} \quad (2)$$

where K, n, Φ_F, J_F are the same as those above-mentioned. Thus, Förster distances were calculated as 33.5 and 44.6 Å for **Py-Per-Py** and **Py-e-Per-e-Py**, respectively.

3.4. Optimized molecular structures

To gain insights into the intramolecular interactions and the electronic structures, theoretical calculations have been performed. The optimized structures are shown in Fig. 6. The highest-occupied molecular orbital (HOMO) and the lowest-unoccupied molecular orbital (LUMO) for the triads obtained by using the same method are also shown in Fig. 6. The HOMO was found to be entirely located on the pyrene-like moieties, while the LUMO was found to be entirely located on the perylene bisimide moieties for both triads. These findings suggest that in the charge-separated state the radical cation is localized on the pyrene moiety, while the radical anion is localized on the perylene bisimide moiety. Moreover, the absence of HOMOs on perylene bisimide and LUMOs on the pyrene-like moiety suggests weak charge-transfer-type interactions between the donor and acceptor entities of the triad in the ground state. It is noted that the HOMO of **Py-e-Per-e-Py** involve the ethynyl group and the phenylene ring. We can safely conclude, therefore, that the pyrene with the ethynyl group and the phenylene ring act cooperatively as a single chromophore and that the corresponding S1 state is delocalized over the entire substituent moiety. It is conceivable that introducing the ethynylene bond into the rod-like pyrene–perylene bisimide system produced a remarkable influence on the photophysical properties.

4. Conclusion

The rod-like pyrene–perylene bisimide triads were synthesized and characterized. The steady-state and time-resolved emission spectroscopy studies gave clear proof that there is energy transfer from **Py*** to the **Per*** in **Py-Per-Py** and **Py-e-Per-e-Py** triads. More-

over, the energy transfer process for the latter is 10-fold faster than that of the former. The pyrene moieties can rotate freely around the connecting ethynylene bond in the **Py-e-Per-e-Py** triad, but only swing in **Py-Per-Py** triad, resulting in differences in the photophysical properties.

Acknowledgement

The authors wish to thank Prof. M. Kira (Tohoku University, Japan) for his helpful discussion.

References

[1] C.-C. Chu, D.M. Bassani, Photochem. Photobiol. Sci. 7 (2008) 521.
[2] A.C. Benniston, A. Harriman, Mater. Today 11 (2008) 26.
[3] H. Tian, Q.-C. Wang, Chem. Soc. Rev. 35 (2006) 361.
[4] V. Balzani, A. Credi, M. Venturi, Molecular Devices and Machines—Concepts and Perspectives for the Nanoworld, Wiley-VCH, Weinheim, 2008.
[5] J.L. Segura, N. Martín, D.M. Guldi, Chem. Soc. Rev. 34 (2005) 31.
[6] S.-C. Lo, P.L. Burn, Chem. Rev. 107 (2007) 1097.
[7] M.R. Wasielewski, Chem. Rev 92 (1992) 435.
[8] F. Vogtle, J.F. Stoddart, M. Shibasaki, Electron and energy transfer, in: M.N. Paddon-Row (Ed.), Stimulating Concepts in Chemistry, Wiley-VCH, New York, 2000, pp. 267–291.
[9] D. Gust, T.A. Moore, A.L. Moore, Acc. Chem. Res. 34 (2001) 40.
[10] D.M. Guldi, Chem. Soc. Rev. 31 (2002) 22.
[11] H.C. Kang, R.P. Haugland, U.S. Patent 5451663, September 19, 1995.
[12] C. Goze, G. Ulrich, L. Charbonnie're, M. Cesario, T. Prange, R. Ziessel, Chem. Eur. J. 9 (2003) 3748.
[13] G.S. Jiao, L.H. Thoresen, K. Burgess, J. Am. Chem. Soc. 125 (2003) 14668.
[14] M.A. Loi, P. Denk, H. Hoppe, H. Neugebauer, C. Winder, D. Meissner, C. Brabec, N.S. Sariciftci, A. Gouloumis, P. Vázquezb, T. Torres, J. Mater. Chem. 13 (2003) 700.
[15] J.E. Mose, Nat. Mater. 4 (2005) 723.
[16] Y. Eichen, G. Nakhmanovich, O. Epshtein, E. Ehrenfreund, J. Phys. Chem. B 104 (2000) 770.
[17] R. Dobrawa, F. Würthner, Chem. Commun. 17 (2002) 1878.
[18] A. Sautter, B.K. Kaletas, D.G. Schmid, R. Dobrawa, M. Zimine, G. Jung, H.M. Ivo, van. Stokkum, L.D. Cola, R.M. Williams, F. Würthner, J. Am. Chem. Soc. 125 (2005) 6719.
[19] A. Herrmann, T. Weil, V. Sinigersky, U.M. Wiesler, T. Vosch, J. Hofkens, F.C. De. Schryver, K. Müllen, Chem. Eur. J. 7 (2001) 4844.
[20] Y. Zhang, Z. Xu, L.Z. Cai, G.Q. Lai, H.X. Qiu, Y.J. Shen, J. Photochem. Photobiol. A 200 (2008) 334.
[21] J.Y. Li, M.L. Peng, L.P. Zhang, L.Z. Wu, B.J. Wang, C.H. Tung, J. Photochem. Photobiol. A 150 (2002) 101.
[22] A. Harriman, G. Izzet, R. Ziessel, J. Am. Chem. Soc. 128 (2006) 10868.
[23] S. Bernhardt, M. Kastler, V. Enkelmann, M. Baumgarten, K. Müllen, Chem. Eur. J. 12 (2006) 6117.
[24] S.W. Yang, A. Elangovan, K.C. Hwang, T.I. Ho, J. Phys. Chem. B 109 (2005) 16628.
[25] A.S.D. Sandanayaka, Y. Araki, O. Ito, G.R. Deviprasad, P.M. Smith, L.M. Rogers, M.E. Zandler, F. D'Souza, Chem. Phys. 325 (2006) 452.
[26] B.K. Kaletas, R. Dobrawa, A. Sautter, F. Würthner, M. Zimine, L.D. Cola, R.M. Williams, J. Phys. Chem. A 108 (2004) 1900.
[27] Y.J. Li, H. Li, Y.L. Li, H.B. Liu, S. Wang, X.R. He, N. Wang, D.B. Zhu, Org. Lett. 7 (2005) 4835.
[28] W. Wolfgang, Ger. Offen. DE. 2237539 19740214, February 14, 1974.
[29] R. Setsu, S. Hirota, S. Mitsuru, Jpn Kokai Tokkyo Koho. JP. 62005672 A 19870112 Showa, January 12, 1987.
[30] J.A. Mikroyannidis, M.M. Stylianakis, M.S. Roy, P. Suresh, G.D. Sharma, J. Power Sources 194 (2009) 1171.
[31] B. Paulson, K. Hamod, P. Eaton, G. Closs, J.R. Miller, J. Phys. Chem. 97 (1993) 13042.
[32] D.I. Schuster, P. Cheng, S.R. Wilson, V. Prokhorenko, M. Katterle, A.R. Holzwarth, S.E. Braslavsky, G. Klihm, R.M. Williams, C.P. Luo, J. Am. Chem. Soc. 121 (1999) 11599.
[33] P. Samori, A. Fechtenkotter, E. Reauther, M.D. Waston, N. Severin, K. Müllen, J.P. Rabe, Adv. Mater. 18 (2006) 1317.
[34] Y.B. Li, J.H. Wan, G.C. Qi, K. Deng, Y.L. Yang, Q.D. Zeng, W. Huang, C. Wang, Chem. Phys. Lett. 474 (2009) 132.
[35] H.Y. Wang, K.Y. Pu, S. Wang, F. Liu, B. Peng, W. Wei, React. Funct. Polym. 69 (2009) 117.
[36] C. Atienza, B. Insuasty, C. Seoane, N. Martín, J. Ramey, G.M.A. Rahmand, D.M. Guldi, J. Mater. Chem. 15 (2005) 124.
[37] D. Dotcheva, M. Klapper, K. Müllen, Macromol. Chem. Phys. 195 (1994) 1905.
[38] M.J. Frisch, G.W. Trucks, H.B. Schlegel, G.E. Scuseria, M.A. Robb, J.R. Cheeseman, J.A. Montgomery Jr., T. Vreven, K.N. Kudin, J.C. Burant, J.M. Millam, S.S. Iyengar, J. Tomasi, V. Barone, B. Mennucci, M. Cossi, G. Scalmani, N. Rega, G.A. Petersson, H. Nakatsuji, M. Hada, M. Ehara, K. Toyota, R. Fukuda, J. Hasegawa, M. Ishida, T. Nakajima, Y. Honda, O. Kitao, H. Nakai, M. Klene, X. Li, J.E. Knox, H.P. Hratchian, J.B. Cross, V. Bakken, C. Adamo, J. Jaramillo, R. Gomperts, R.E. Stratmann, O. Yazyev, A.J. Austin, R. Cammi, C. Pomelli, J.W. Ochterski, P.Y. Ayala, K. Morokuma, G.A. Voth, P. Salvador, J.J. Dannenberg, V.G. Zakrzewski, S. Dapprich, A.D. Daniels, M.C. Strain, O. Farkas, D.K. Malick, A.D. Rabuck, K. Raghavachari, J.B. Foresman, J.V. Ortiz, Q. Cui, A.G. Baboul, S. Clifford, J. Cioslowski, B.B. Stefanov, G. Liu, A. Liashenko, P. Piskorz, I. Komaromi, R.L. Martin, D.J. Fox, T. Keith, M.A. Al-Laham, C.Y. Peng, A. Nanayakkara, M. Challacombe, P.M.W. Gill, B. Johnson, W. Chen, M.W. Wong, C. Gonzalez, J.A. Pople, Gaussian 03, Revision D.01, Gaussian Inc., Wallingford, CT, 2004.
[39] M. Hissler, A. Harriman, A. Khatyr, R. Ziessel, Chem. Eur. J. 5 (1999) 3366.
[40] A.C. Benniston, A. Harriman, D.J. Lawrie, S.A. Rostron, Eur. J. Org. Chem. 10 (2004) 2272.
[41] K. Sonogashira, Y. Tohda, N. Hagihara, Tetrahedron Lett. 16 (1975) 4467.
[42] C.S. Wang, L.O. Palsson, A.S. Batsanov, M.R. Bryce, J. Am. Chem. Soc. 128 (2006) 3789.
[43] R. Gvishi, R. Reisfeld, Z. Burshtein, Chem. Phys. Lett. 213 (1993) 338.
[44] D. Liu, S. De Feyter, M. Cotlet, A. Stefan, U.M. Wiesler, A. Herrmann, D. Grebel-Koehler, J. Qu, K. Mullen, F.C. De Schryver, Macromolecules 36 (2003) 5918.
[45] M.P. O'Neil, M.P. Niemczyk, W.A. Svec, D. Gosztola, G.L. Gaines, M.R. Wasielewski, Science 257 (1992) 63.
[46] D. Gosztola, M.P. Niemczyk, M.R. Wasielewski, J. Am. Chem. Soc. 120 (1998) 5118.
[47] S. Prathapan, S. Ik Yang, J. Seth, M.A. Miller, D.F. Bocian, D. Holten, J.S. Lindsey, J. Phys. Chem. B 105 (2001) 8237.
[48] F. Würthner, Chem. Commun. 14 (2004) 1564.
[49] M.J. Ahrens, M.J. Tauber, M.R. Wasielewski, J. Org. Chem. 71 (2006) 2107.
[50] T. Förster, Ann. Phys. 2 (1948) 55.